Adıyaman University Journal of Science
https://dergipark.org.tr/en/pub/adyujsci
DergiPark AKADEMİK
ISSN 2147-1630
e-ISSN 2146-586X

Theoretical Prediction of Pressure-Dependent Elastic, Ultrasonic Properties, and Thermo-Physical Properties of Zinc Metal

Prashant SRIVASTAV[1,*], Adwitiya YADAV[1], Pramod Kumar YADAWA[1]

[1]*Department of Physics, Prof. Rajendra Singh (RajjuBhaiya) Institute of Physical Sciences for Study and Research, V.B.S. Purvanchal University, 222003, Jaunpur, India*
Srivastavprashant001@gmail.com, ORCID: 0000-0003-4596-6258
[1]*Department of Physics, Prof. Rajendra Singh (RajjuBhaiya) Institute of Physical Sciences for Study and Research, V.B.S. Purvanchal University, 222003, Jaunpur, India*
Adwitiya94@gmail.com, ORCID: 0009-0009-0978-6111
[1]*Department of Physics, Prof. Rajendra Singh (RajjuBhaiya) Institute of Physical Sciences for Study and Research, V.B.S. Purvanchal University, 22200, Jaunpur, India*
pkyadawa@gmail.com, ORCID: 0000-0002-9525-2205

Received: 26.04.2025 **Accepted:** 17.12.2025 **Published:** 31.12.2025

Abstract

This research uses the Lennard-Jones potential model to study the mechanical, thermodynamic, and elastic properties of zinc metal when pressure is applied between 0 and 120 GPa. The obtained elastic and mechanical properties agreed with the further theoretical consequences. The evaluated mechanical properties show that Zn metal is mechanically stable, and elastic constants increase up to 60 GPa. An investigation of the elastic modulus indicates that Zn metal possesses a large shear modulus, bulk modulus, and Young's modulus. The better mechanical properties classify that metal as a likely candidate for a superhard metal under high pressure. As a result of evaluating the B/G and Poisson's ratio, it is predicted that Zn metal possesses brittle behaviour from 0 to 120 GPa pressure range, and the increase in pressure can reduce its brittleness. Finally, the thermal properties, including heat capacity per unit volume (C_V) and Θ_D (Debye temperature), are obtained under a 0-120 GPa pressure range. The pressure-

* Corresponding Author DOI: 10.37094/adyujsci.1683623

dependent ultrasonic velocities and attenuation of this metal, Zn, have been evaluated. This zinc metal exhibits enhanced structural stability at higher pressures (80–120 GPa), and the minimum ultrasonic attenuation observed at 120 GPa indicates improved ductility.

Keywords: Zinc; Elastic properties; Mechanical properties; Ultrasonic properties; Thermal properties.

Çinko Metalinin Basınca Bağlı Elastik, Ultrasonik ve Termo-Fiziksel Özelliklerinin Teorik Tahmini

Öz

Bu araştırma, 0 ile 120 GPa arasında basınç uygulandığında çinko metalinin mekanik, termodinamik ve elastik özelliklerini incelemek için Lennard-Jones potansiyel modelini kullanmaktadır. Elde edilen elastik özellikler ve mekanik özellikler, diğer teorik sonuçlarla uyuşmaktadır. Değerlendirilen mekanik özellikler, Zn metalinin mekanik olarak kararlı olduğunu ve elastik sabitlerinin 60 GPa'ya kadar arttığını göstermektedir. Elastik modülünün incelenmesi, Zn metalinin büyük bir kayma modülüne, hacim modülüne ve Young modülüne sahip olduğunu göstermektedir. Daha iyi mekanik özellikler, bu metali yüksek basınç altında süper sert bir metal için olası bir aday olarak sınıflandırır. B/G ve Poisson oranının değerlendirilmesi sonucunda, Zn metalinin 0 ila 120 GPa basınç aralığında kırılgan davranışa sahip olduğu ve basınç artışlarının kırılganlığını azaltabileceği öngörülmektedir. Son olarak, birim hacim başına ısı kapasitesi (C_V) ve Θ_D (Debye sıcaklığı) dahil olmak üzere termal özellikler, 0-120 GPa basınç aralığında elde edilmektedir. Bu çinko metali, yüksek basınçlarda (80-120 GPa) gelişmiş yapısal kararlılık sergilemekte olup, 120 GPa'da gözlemlenen minimum ultrasonik zayıflama, gelişmiş süneklik göstergesidir.

Anahtar Kelimeler: Çinko; Elastik özellikler; Mekanik özellikler; Ultrasonik özellikler; Termal özellikler.

1. Introduction

The ultrasonic Non-destructive tools are well-known for analyzing the characteristics of this metal by calculating ultrasonic attenuation. The good physical and chemical characteristics of the elemental metal establish it as a valuable element among metals. One of the fundamental metals, Zinc, has a wide range of industrial uses [1-3]. The elastic behavior and wave propagation in solids can be adequately described by the second-order elastic coefficients (SOECs) [4, 5], whereas the strain properties of that materials involve the evaluation of the third-order elastic constants (TOECs). Essentially, the SOECs and TOECs explain the way materials react to linear

and nonlinear elasticity, accordingly [6, 7]. It has an important function in the composition of several different alloys, including Ni, Ag, and Cu. Zn is distinctive among the basic metals in terms of crystallography. It uses the universal HCP shape observed in the crystalline structure of metals. Metal that has a bluish-white color and a polished appearance is zinc. While it is brittle, at the increases in temperature it exhibits good malleability and ductility. The symbol Zn stands for zinc, which has the atomic number 30. It corresponds to the periodic table's d-block, period 4, and group 12 subgroups. Its electronic structure, [Ar] $3d^{lO}4s^2$, shows that the d band is filled and that complex d-band/s-band electronic interactions are unlikely [8, 9]. Zinc has a single crystal structure between absolute zero and its melting point (692 K); hence, no surprising temperature discontinuities occur in its solid-state properties. Nevertheless, its behavior is comparatively complex from an elastic perspective [10]. A few fundamental ideas are presented to better comprehend zinc's elasticity [11]. Zinc is commonly employed. Galvanized iron and steel die castings, solders, and alloys are a few examples of uses that are well-known [12]. One of the most popular and practical zinc alloys is certainly brass (zinc-copper alloys).

In the present investigation, the elastic, mechanical, and ultrasonic properties of Zn metal have been studied using the Lennard-Jones (LJ) interaction potential approach. The Lennard-Jones potential has been widely employed in the literature to describe interatomic interactions in metals and intermetallic compounds, particularly for evaluating elastic constants, thermophysical parameters, and ultrasonic properties under pressure. This semi-empirical potential effectively captures both the short-range repulsive and long-range attractive interactions between atoms and has been successfully applied to hexagonal close-packed metals in earlier studies. In this work, the Lennard-Jones potential framework is extended to systematically investigate the pressure-dependent elastic stability, ultrasonic velocities, attenuation, and thermophysical behavior of Zn metal over a wide pressure range of 0–120 GPa.

2. Computational Methodology

The higher-order elastic coefficients (SOECs and TOECs) are essential variables because they should be connected to several thermophysical features that help in appreciating the condensed performance of metal. To establish Zn metal's higher-order nonlinear elastic coefficients, the basic interaction potential model approach will be used, eliminating the many obstacles and approximations of the first-principles computation model. By considering the Lennard-Jones potential as a potential for several body interactions, the subsequent formulas should be used to determine the SOECs and TOECs of a metal with a HCP structure [13, 14].

$$\left.\begin{array}{ll} C_{11} = 24.1\ \mathrm{p}^4 C' & C_{12} = 5.918\ \mathrm{p}^4 C' \\ C_{13} = 1.925\ \mathrm{p}^6 C' & C_{33} = 3.464\ \mathrm{p}^8 C' \\ C_{44} = 2.309 p^4 C' & C_{66} = 9.851\ \mathrm{p}^4 C' \end{array}\right\} \quad (1)$$

$$C_{111} = 126.9p^2B + 8.853p^4C' \qquad C_{112} = 19.168p^2B - 1.61p^4C'$$

$$C_{113} = 1.924p^4B + 1.155p^6C' \qquad C_{123} = 1.617p^4B - 1.155p^6C'$$

$$C_{133} = 3.695p^6B \qquad C_{155} = 1.539p^4B$$

$$C_{144} = 2.309p^4B \qquad C_{344} = 3.464p^6B$$

$$C_{222} = 101.039p^2B + 9.007p^4C' \quad C_{333} = 5.196p^8B$$

The harmonic parameter (χ), also the enharmonic constraint (Ψ) are obtained using the 'a' (basal plane distance), 'p=c/a' (axial ratio), with proper SOEC constants are using these equations.

$$\chi = (1/8)[\{nb_0\ (n-m)\}/\{\ \mathrm{a}^{n+4}\}] \quad (2)$$

$$\psi = -\chi\ /\{6\ \mathrm{a}^2(m+n+6)\} \quad (3)$$

The SOECs under the Voigt–Reuss–Hill (VRH) estimate [15] is well-known to compute various mechanical parameters, such as the Young's modulus (Y), shear modulus (G), Poisson's ratio (σ), Pugh's ratio (B/G) bulk modulus (B) [16]. Using the VRH approximation, the expression for the characteristic bulk modulus and shear modulus is provided as:

$$\left.\begin{array}{l} M = C_{11} + C_{12} + 2C_{33} - 4C_{13}, \mathrm{C}^2 = (C_{11} + C_{12})C_{33} - 4C_{13} + C^2{}_{13}; \\ B_R = \frac{C^2}{M}; \mathrm{B}_V = \frac{2(C_{11}+C_{12})+4C_{13}+C_{33}}{9}; \\ G_V = \frac{M+12(C_{44}+C_{66})}{30}; \mathrm{G}_R = \frac{5C^2C_{44}C_{66}}{2[3B_VC_{44}C_{66}+C^2(C_{44}+C_{66})]}; \\ Y = \frac{9GB}{G+3B}; \quad \mathrm{B} = \frac{B_V+B_R}{2}; \quad \mathrm{G} = \frac{G_V+G_R}{2}; \sigma = \frac{\mathrm{3B\text{-}2G}}{2(\mathrm{3B}+G)} \end{array}\right\} \quad (4)$$

There are one longitudinal (V_L) and two shear acoustical wave velocities (V_{S1}, V_{S2}). These velocities, which exist in hexagonal materials, are closely related to the SOECs and material density. The following formulas can be used to determine the velocities [17].

$$\left.\begin{aligned} V_L^2 &= \{C_{33}\cos^2\theta + C_{11}\sin^2\theta + C_{44} \\ &\quad +\{[C_{11}\sin^2\theta - C_{33}\cos^2\theta \\ &\quad +C_{44}(\cos^2\theta - \sin^2\theta)]^2 \\ &\quad +4\cos^2\theta\sin^2\theta\,(C_{13}+C_{44})^2\}^{1/2}\}/2\rho \\ V_{S1}^2 &= \{C_{33}\cos^2\theta + C_{11}\sin^2\theta \\ &\quad +C_{44} - \{[C_{11}\sin^2\theta - C_{33}\cos^2\theta \\ &\quad +C_{44}(\cos^2\theta - \sin^2\theta)]^2 \\ &\quad +4\cos^2\theta\sin^2\theta\,(C_{13}+C_{44})^2\}^{1/2}\}/2\rho \\ V_{S2}^2 &= \{C_{44}\cos^2\theta + C_{66}\sin^2\theta\}/\rho \end{aligned}\right\} \quad (5)$$

The longitudinal wave, quasi-shear wave, and shear wave velocities can be represented by the variables V_L, V_{S2}, and V_{S3}. The values ρ and θ represent the material's density and angle concerning the crystal's unique axis, or z-axis. We can use the following expressions to calculate the density and ultrasonic velocities of hexagonal-structured Zn metal [18, 19]

$$\rho = \frac{2Mn}{3\sqrt{3}a^2CN_A} \quad (6)$$

Molecular weight, Avogadro number, and number of atoms per unit cell are represented by the symbols M, N_A, and n, respectively.

Considering that the Debye average velocity is interconnected to elastic coefficients using V_L, V_{S1}, and V_{S2}, it is an essential measure in low-temperature physics. In favor of wave propagation at any angle with the z-axis, the Debye average velocity (V_D) has been defined as [20, 21].

$$V_D = \left[\frac{1}{3}\left(\frac{1}{V_L^3} + \frac{1}{V_{s1}^3} + \frac{1}{V_{s2}^3}\right)\right]^{-1/3} \quad (7)$$

The Debye temperature (θ_D) of the metal is influenced by the Debye average velocity (V_D). Debye average velocity, expressed as, directly relates to variations in Debye temperature [22].

$$\theta_D = \frac{\hbar V_D\left(6\pi^2 n_a\right)^{1/3}}{K_B} \quad (8)$$

Here, the Boltzmann Constant is symbolized by K_B, the atom concentration is denoted by n_a, and the quantum of action, $\hbar$, is defined as Planck's constant divided by 2π. The thermal distribution of phonons occurs during the ultrasonic wave. The thermal relaxation time (τ), which can be calculated using the following formula, is the duration of time expected for the thermal phonons to return to equilibrium [23, 24]:

$$\tau = \tau_S = \tau_L/2 = \frac{3k}{C_V V_D^2} \tag{9}$$

K in this case signifies the thermal conductivity. The metal thermal conductivity [25] can be determined through:

$$k = k_B V_D \left[\frac{M}{n\rho N_A}\right]^{-\frac{2}{3}} \tag{10}$$

The total consequence of ultrasonic attenuation $(A/f^2)_{Total}$, caused by the thermoelastic loss and Akhieser losses exhibited in the longitudinal (V_L), shear mode of propagation can be calculated as [26]:

$$\left\{\frac{\alpha}{f^2}\right\}_{Total} = \left\{\frac{\alpha}{f^2}\right\}_{Th} + \left\{\frac{\alpha}{f^2}\right\}_{Long} + \left\{\frac{\alpha}{f^2}\right\}_{Shear} \tag{11}$$

Where $\left\{\frac{\alpha}{f^2}\right\}_{Th}$ is the thermo-elastic loss, $\left\{\frac{\alpha}{f^2}\right\}_{long}$ and $\left\{\frac{\alpha}{f^2}\right\}_{shear}$. The ultrasonic attenuation coefficients for the longitudinal wave (V_L) and shear waves, respectively.

3. Results and Discussion

3.1. Elastic and Mechanical Parameters

In the present research, we have computed the elastic coefficients (6 -SOECs and 10-TOECs) by an interaction potential model, and lattice characteristics for the Zn element, "a" (lattice parameter) and "c/a" (axial ratio) are obtained in Fig. 1 [12].

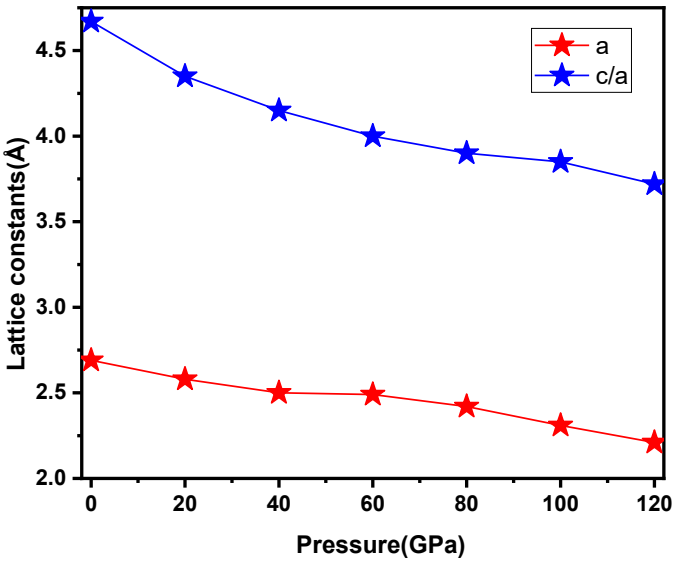

Figure 1: Lattice parameter for Zn under pressure

The value of b_0 is taken at $2.16x10^{-64}$ erg cm^7 for the Zn element. The values of the higher-order elastic coefficients (second and third-order) of the Zinc element under the 0-120 GPa are obtained in Figs. 2 and 3 accordingly.

Elastic parameters can also provide an improved knowledge of macroscopic mechanical characteristics and contribute to evaluating a metal's hardness. Whereas the measurement value of C_{13} increases slightly less with 0-120 GPa in Fig. 2, the value of C_{11} increases with increasing pressure. Although the values of C_{12} and C_{44} increase slightly less with 0-120 GPa in Fig. 2, the value of C_{33} increases with 0-120 GPa.

Figure 3 illustrates the evaluated TOEC values at 0-120 GPa. TOECs with negative values signify strain within the solid. As a result, the model used to investigate higher-order elastic coefficients is acceptable [27, 28] using Eqns. (1)-(2). For HCP structure material stability, the five different SOECs (C_{ij}, namely C_{11}, C_{12}, C_{13}, C_{33}, C_{44}) satisfy Born-Huang's norms [29, 30]. This Zn element is mechanically stable at 0-120 GPa because it is evident that the positive elastic constant values satisfy Born-mechanical Huang's stability constraints.

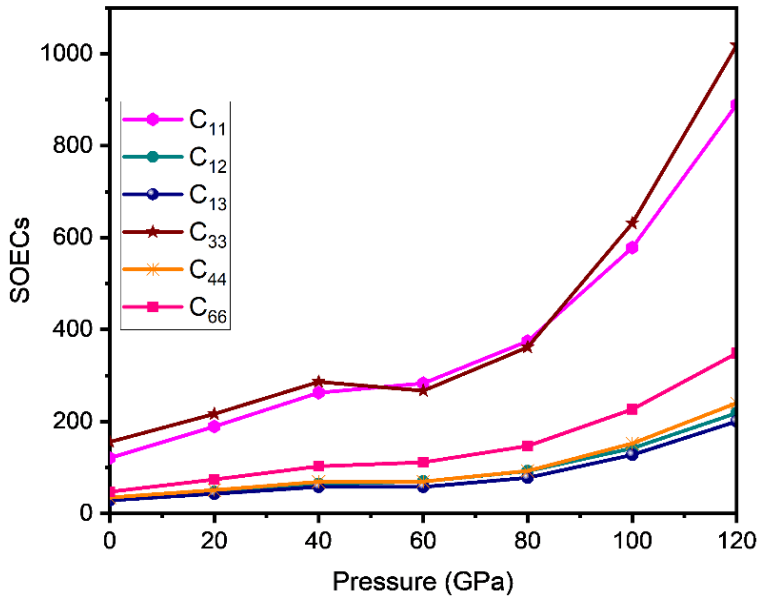

Figure 2: The SOECs of Zn under pressure

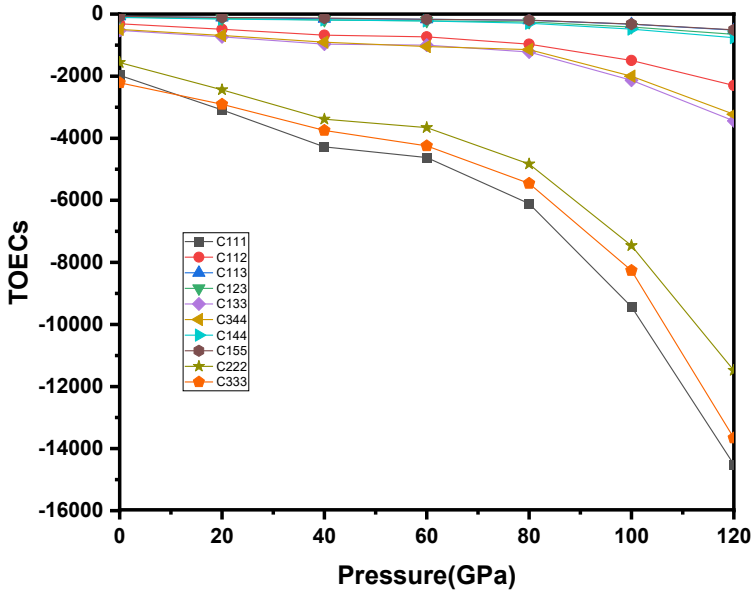

Figure 3: TOECs of Zn under pressure

The computed HOECs are closely related to the fundamental solid-state phenomenon. It is used to evaluate the mechanical properties under the Voigt approximation and the Reuss approximation. In this approximation, Voigt-Reuss' constants (M and C^2) followed by the Shear modulus (G), Young's modulus (Y), toughness (G/B), bulk modulus (B), Pugh's ratio (B/G), and Poisson's ratio (σ) at pressure ranges of 0-120 GPa have been calculated and shown in Table 1.

Table 1: M, C^2, B, G, Y, G/B, B/G, and σ of Zn under the Pressure range 0-120 GPa

Pressure (GPa)	M	C^2	B	G	Y	G/B	B/G	σ
0	346	24215	66	43	107	0.6	1.5	0.23
20	498	52714	100	65	162	0.6	1.5	0.22
40	655	96714	137	89	221	0.6	1.5	0.23
60	668	97350	141	92	227	0.6	1.5	0.23
80	879	174453	188	123	303	0.6	1.5	0.23
100	1473	470568	303	198	488	0.6	1.5	0.23
120	2343	1168397	473	309	763	0.6	1.5	0.23

Within the Voigt–Reuss–Hill (VRH) approximation, the elastic constants M and C^2 represent effective elastic stiffness parameters derived from the second-order elastic constants. The parameter M corresponds to the longitudinal elastic stiffness associated with axial deformation, whereas C^2 represents the effective shear-related elastic constant obtained from the Voigt–Reuss averaging scheme. These parameters play an important role in determining the bulk modulus (B), shear modulus (G), and Young's modulus (Y) of Zn metal under pressure. The

pressure dependence of M and C^2, as presented in Table 1, reflects the enhancement of elastic stiffness and resistance to deformation with increasing pressure. The values of B, Y, and G for Zn metal are observed to increase with pressure range 0-120 GPa. Our calculated bulk modulus results up to zero GPa for *hcp*-Zn have similar trends to those reported at 126 GPa by K. Takemura [12]. The ratio of G/B provides insight into the bonding characteristics of materials. The obtained G/B and B/G values for Zn metal indicate a predominantly metallic bonding nature, with pressure-induced strengthening of interatomic interactions [31]. This ratio helps predict the bonding unique features of compounds, as well as ratios B/G and σ provide insights into the materials' brittleness and ductility. Materials with $\sigma=0.23\leq0.26$ and $B/G = 1.52\leq1.75$ are typically considered brittle, or else they are ductile in nature. Our results for B/G indicate that the element zinc is brittle at pressures between 0 and 120 GPa because it is under its critical levels. The value of σ, which should be perfectly less than 0.5 for elastic and stable metal, is found to be within an acceptable range for Zn.

The Density of Zn element is increasing with increasing pressure, and the volume of Zn element is decreasing with increasing pressure, are shown in Fig. 4.

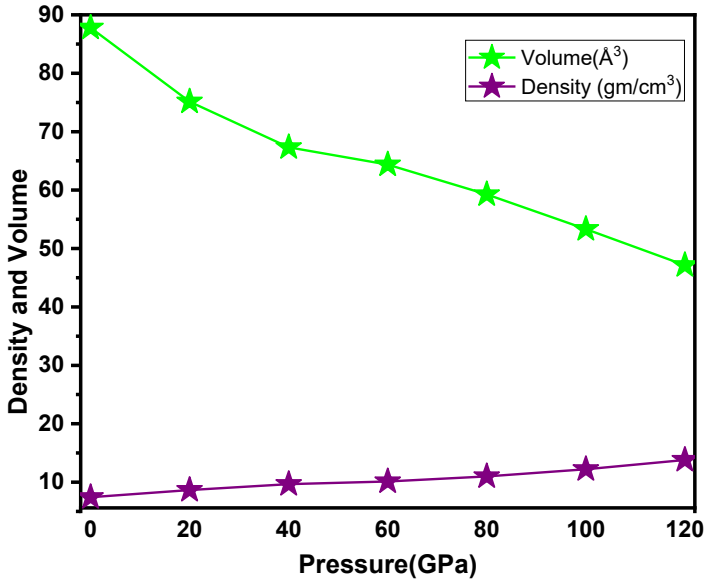

Figure 4: Volume and Density of Zn under pressure

3.2. Ultrasonic Velocity

Figures 5-8 show the angular correlations of ultrasonic velocities (V_L, V_{S1}, V_{S2}, V_D) at various pressures along the z-axis of the Zn metal. In Figs. 5 and 6, the z-axis of the Zinc correlates directly to the minima and maxima of the ultrasonic velocities V_L and V_{S1} of the Zn metal. In Fig. 7, V_{S2} rises through the angle away along the z-direction. The combined effects of SOECs and ρ

(density) are held responsible in favor of the uncharacteristic behavior of θ(angle) θ-dependent velocity. The existence of angle (θ)-dependent velocities (V) curves in this effort is comparable to that discovered for other HCP metals. Hence, the θ-dependence of the velocities in metal is acceptable.

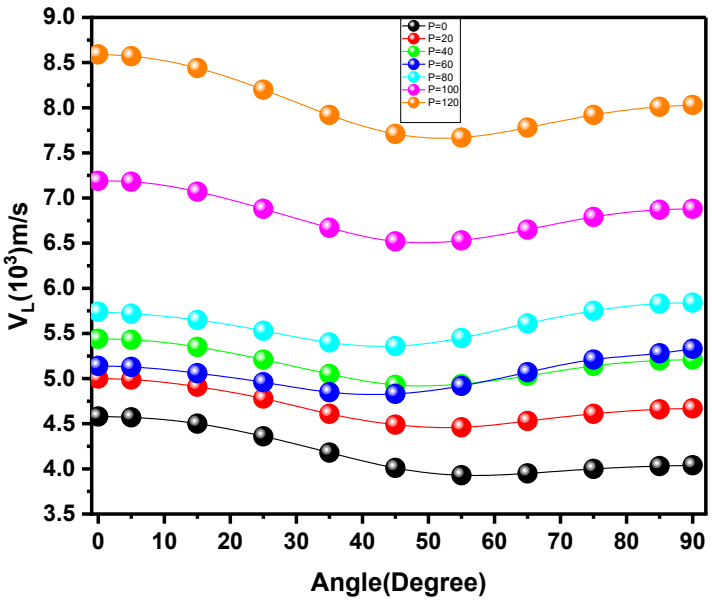

Figure 5: Different pressure and angle-dependent ultrasonic velocity V_L of Zn

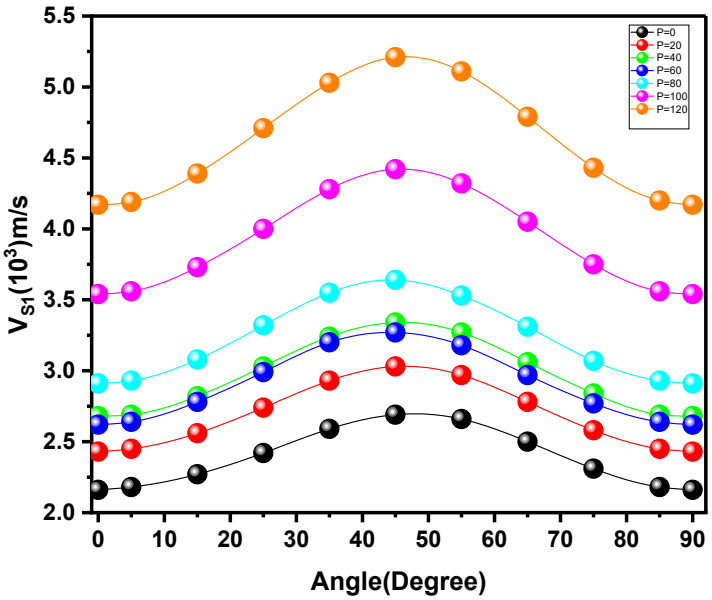

Figure 6: Different pressure and angle-dependent ultrasonic velocity V_{S1} of Zn

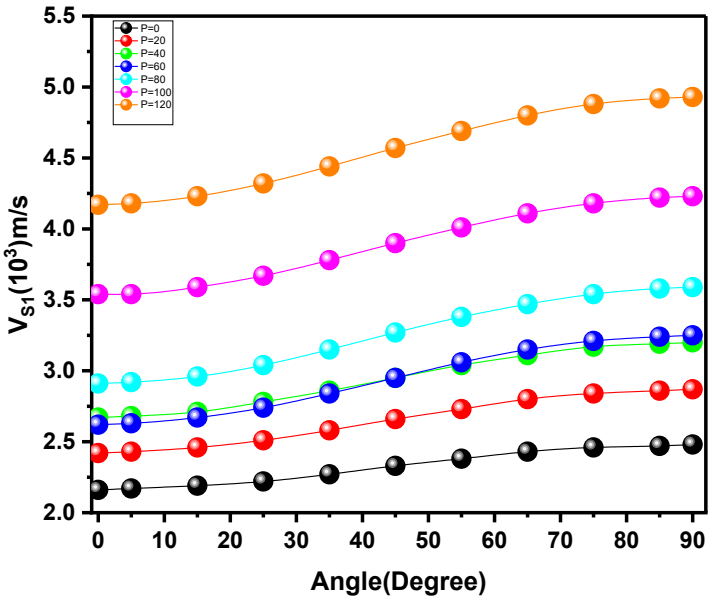

Figure 7: Different pressure and angle-dependent ultrasonic velocity V_{S2} of Zn

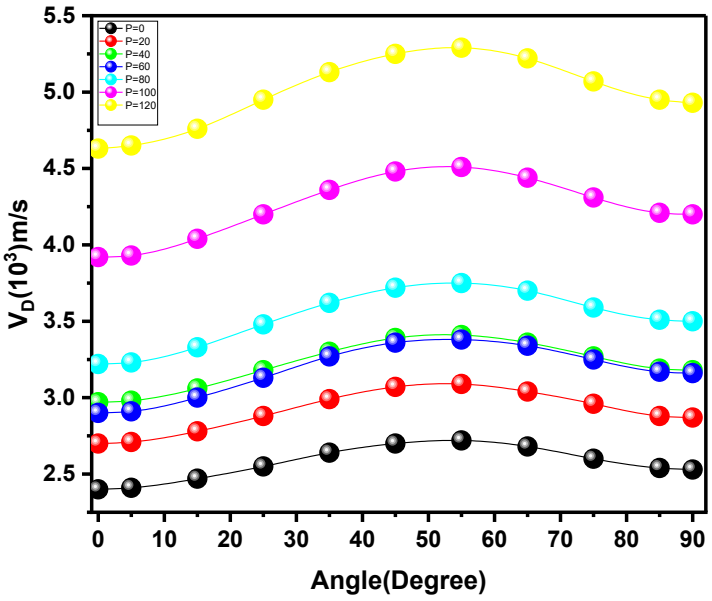

Figure 8: Different pressure and angle-dependent Debye average velocity, V_D of Zn

Figure 8 shows the variance of the Debye average velocity (V_D) as it depends upon θ with the unique axis. When utilizing the ultrasonic velocities V_L, V_{S1}, and V_{S2} for Zn, V_D is accomplished. Its maximum value reaches at 50^0 and it increases with angle (θ).

3.3. Thermal Properties

Thermal conductivity has been calculated with Eqn. (10). The thermal properties of Zn metal under pressure have been evaluated using the elastic and ultrasonic parameters discussed above. The thermal conductivity (κ) of Zn metal has been calculated using Eqn. (10) over the

pressure range of 0–120 GPa, and the obtained results are presented in Fig. 9. It is evident from Fig. 9 that the thermal conductivity of Zn increases monotonically with increasing pressure. This behavior can be attributed to the pressure-induced enhancement of lattice stiffness and phonon transport within the crystal structure.

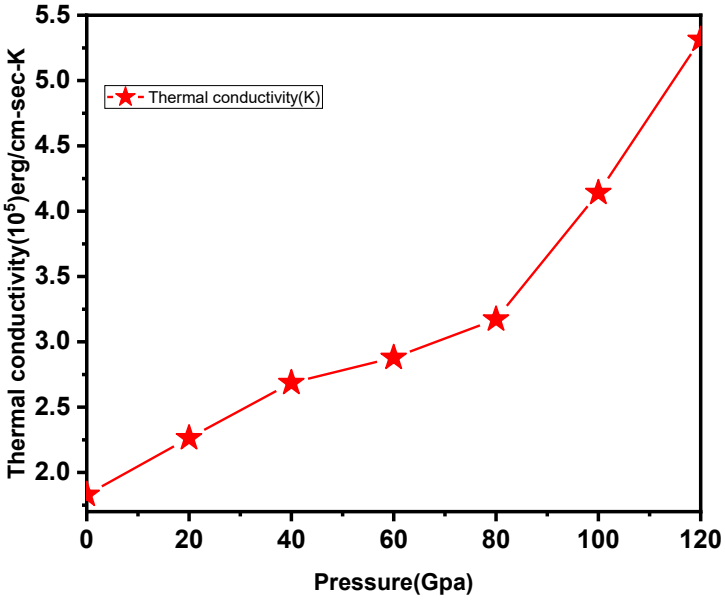

Figure 9: Thermal conductivity (k_{min}) of Zn under pressure

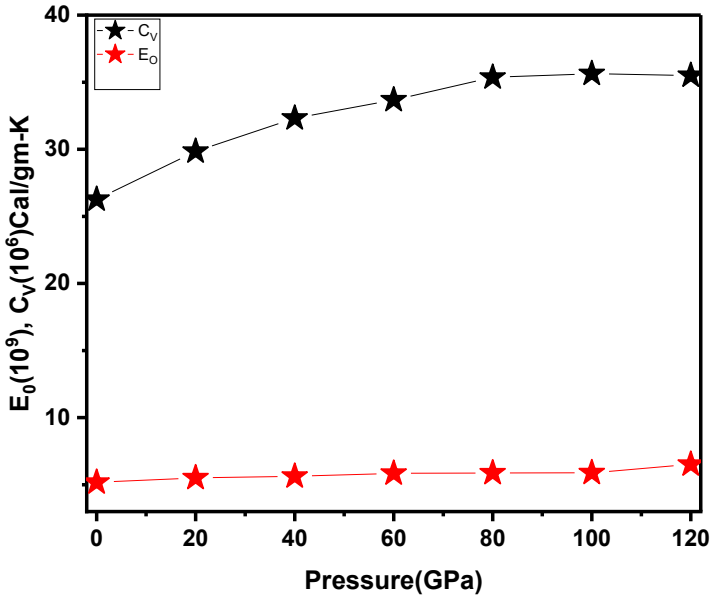

Figure 10: The specific heat per unit volume (C_V) and also the energy density (E_0) of Zn at 0-120 GPa

The specific heat at constant volume (C_V) and the energy density (E_0) of Zn metal as functions of pressure are shown in Fig. 10. The specific heat c_v has been evaluated within the framework of the Debye model. It is observed that c_v increases gradually with increasing pressure

from 0 to 120 GPa. This increase in c_v reflects the modification of phonon spectra due to pressure-dependent lattice compression.

The energy density (E_0) also exhibits an increasing trend with pressure, as illustrated in Fig. 10. The values of E_0 have been obtained using standard data from the AIP Handbook [32]. Since the Debye temperature (θ_D) is inversely related to the specific heat at constant volume, θ_D and C_V exhibit opposite trends with pressure. This inverse relationship is clearly reflected in Fig. 10, indicating the consistency of the obtained thermophysical parameters. The angle and pressure-dependent "τ" (thermal relaxation) is considered through Eqn. (9) at 0-120 GPa.

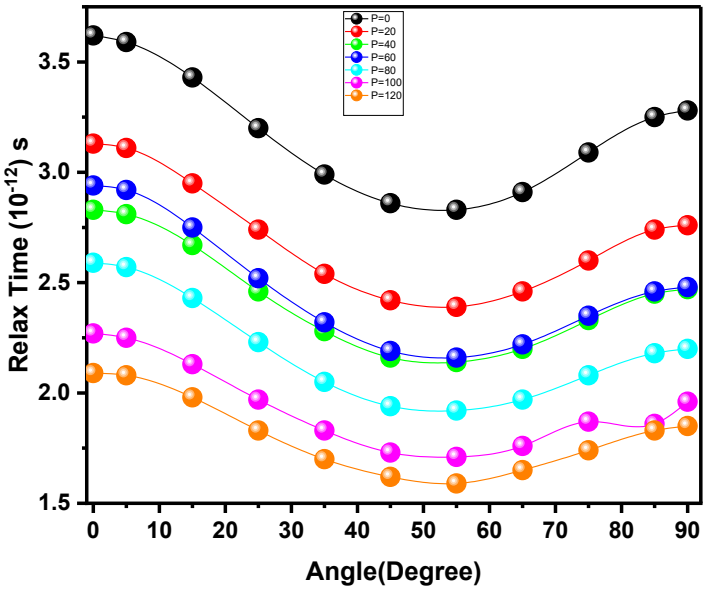

Figure 11: Angle and different pressure (0-120 GPa) dependent relaxation time of Zn

The angle and pressure dependence of thermal relaxation time is obtained in Fig. 11. In Fig. 11, the thermal relaxation time is of the Order 10^{-12} picoseconds. This indicates that Zinc has an intermetallic nature. Thus, thermal conductivity ($\tau \propto k$) has a definite impact on Zn thermal relaxation time. p-p (phonon-phonon) interaction and "τ" thermal relaxation processes induce ultrasonic attenuation, as demonstrated by the shortest computation time for the thermal phonon equilibrium distribution for wave propagation ($\theta = 50^{\circ}$).

3.4. Ultrasonic Attenuation Based on Thermal Relaxation Events and Phonon-Phonon (p-p) Interaction

In analyzing the $\left\{\frac{\alpha}{f^2}\right\}_{Th}$ ultrasonic attenuation, it was assumed that the waves flow along the z-axis of the metal Zn. Attenuation coefficients are linear over frequency squared (α^2) for $\left\{\frac{\alpha}{f^2}\right\}_{long}$

(longitudinal wave) and for,$\left\{\frac{\alpha}{f^2}\right\}_{shear}$ (shear wave) under condition $\alpha\tau<<1$ at 0-120 GPa is calculated using Eqn. (11) and obtained in Table 2. The thermo-elastic loss by frequency squared $(\alpha/f^2)_{th}$ is calculated using Eqn. (11) and the Table 2 illustrates the ultrasonic attenuation value resulting from the thermoelastic relaxation mechanism $(\alpha/f^2)_{th}$.

Table. 2: $\left\{\frac{\alpha}{f^2}\right\}_{Th}$,$\left\{\frac{\alpha}{f^2}\right\}_{long}$,$\left\{\frac{\alpha}{f^2}\right\}_{shear}$ and $\left\{\frac{\alpha}{f^2}\right\}_{Total}$ of Zn at a pressure range of 0-120 GPa

Pressue (GPa)	$\left\{\frac{\alpha}{f^2}\right\}_{Th}$ $(10^{-21})Nps^2m^{-1}$	$\left\{\frac{\alpha}{f^2}\right\}_{long}$ $(10^{-18})Nps^2m^{-1}$	$\left\{\frac{\alpha}{f^2}\right\}_{shear}$ $(10^{-18})Nps^2m^{-1}$	$\left\{\frac{\alpha}{f^2}\right\}_{Total}$ $(10^{-18})Nps^2m^{-1}$
0	3.144	2.909	1.887	4.796
20	2.309	2.044	0.463	2.507
40	2.179	1.879	0.199	2.078
60	1.639	1.379	0.147	1.526
80	1.322	1.072	0.082	1.154
100	0.496	0.057	0.052	0.453
120	0.228	0.032	0.032	0.168

The $\left(\alpha/_{f^2}\right) akh \propto D, E_0 and\ V^{-3}$using Eqn. (11). Thus, in the Zn compound, E_0 and K have a considerable impact on Akhieser losses. The results of $(\alpha/f^2)_{Akh}$have been compared through our recent studies.

As shown in Table 2, the thermo-elastic loss $(\alpha/f^2)_{th}$ (e.g., 0.032×10^{-18} Nps^2m^{-1} at 120 GPa) is significantly smaller than the corresponding Akhieser loss (0.168×10^{-18} Nps^2m^{-1}), indicating that phonon–phonon interaction dominates ultrasonic attenuation. At all pressures, the thermo-elastic attenuation remains at least one order of magnitude lower than the Akhieser attenuation, confirming the dominance of phonon–phonon interaction mechanisms indicating that the p-p interaction mechanism-induced ultrasonic attenuation dominates over the thermo-elastic loss. Total attenuation is essentially driven by two variables, namely thermal energy density and thermal conductivity. Thus, although zinc metal is the least ductile, Zn shows its purest form at higher pressures and shows additional ductility, as shown by the minimal attenuation. Hence, the Zn compound will have the lowest impurity content at 0-120 GPa.

4. Conclusion

Based on the above discussion, the following conclusions are drawn:

- The standard calculation technique for evaluating higher-order elastic coefficients of hexagonal Zn metal, based on the Lennard–Jones potential model, is found to be applicable over the pressure range of 0–120 GPa.

- The evaluated elastic properties indicate that Zn metal remains mechanically stable throughout the entire pressure range of 0–120 GPa.

- The mechanical properties of Zn metal are significantly enhanced at higher pressures, particularly at 120 GPa. The obtained elastic moduli indicate a predominantly metallic bonding character in Zn metal, with pressure-induced strengthening of interatomic interactions. Moreover, Zn metal exhibits improved structural stability and increased ductility at higher pressures, as confirmed by the observed minimum ultrasonic attenuation.

- The "τ" of Zn metal is established to the order of picoseconds, defending its inter-metallic nature. The smallest significance of 'τ' along = 50^0 at all temperatures indicates that the time required to re-establish the equilibrium distribution of phonons for wave propagation in the z-direction will be the shortest.

- The total ultrasonic attenuation is dominated by the phonon–phonon (p–p) interaction mechanism, while the thermo-elastic loss remains comparatively small. Thermal conductivity (κ) plays a crucial role in governing ultrasonic attenuation. Based on ultrasonic attenuation behavior, materials may be classified as metallic, semiconducting, intermediate-valence, or dielectric in nature.

This study provides a reliable theoretical framework for the computational and non-destructive characterization of metals under pressure. The present results may serve as a foundation for future investigations into the elastic, ultrasonic, and thermophysical properties of other metallic systems.

Acknowledgements

The authors gratefully acknowledge the financial support from the Center of Excellence grant from the Department of Higher Education, Government of Uttar Pradesh.

References

[1] McCammon, R.D., White, G.K., *Thermal Expansion at Low Temperatures of Hexagonal Metals: Mg, Zn and Cd*, Philosophical Magazine, 11(114), 1125–1134, 1965.

[2] Vaidya, S.N., Kenned, G.C., *Compressibility of 18 Metals to 45 kbar,* Journal of Physics and Chemistry of Solids, 31, 2329–2345, 1970.

[3] McQueen, R.G., Marsh, S.P., *Equation of State for Nineteen Metallic Elements from Shock-Wave Measurements to Two Megabars*, Journal of Applied Physics, 31, 1253−1269, 1960.

[4] Akella, J., Ganguly, J., Grover, R., Kennedy, G., *Melting of Lead and Zinc to 60 kbar*, Journal of Physics and Chemistry of Solids, 34, 631−636, 1973.

[5] Born, M., Huang, K., Lax, M., *Dynamical theory of crystal lattices*, American Journal of Physics, 23(7), 474, 1955.

[6] Wallace, D.C., *Thermoelastic Theory of Stressed Crystals and Higher-Order Elastic Constants*, Solid State Physics, 25, 301−404, 1970.

[7] Brugger, K., *Thermodynamic definition of higher order elastic coefficients*, Physical Review, 133, 1611–1612, 1964.

[8] Errandonea, D., MacLeod, S.G., Ruiz-Fuertes, J., Burakovsky, L., McMahon, M.I., Wilson, C.W. et al., *High-Pressure/High-Temperature Phase Diagram of Zinc*, Journal of Physics: Condensed Matter, 30, 295402, 2018.

[9] Schirber, J.E., *Effect of Pressure and Magnetic Field on the Connectivity of the Fermi Surface of Zinc*, Physical Review, 140, 2065−2075, 1965.

[10] O'Sullivan, W.J., Schirber, J.E., *Pressure Dependence of the Low-Frequency Haas—Van Alphen Oscillations in Zn*, Physical Review, 151, 484−494, 1966.

[11] Lynch, R.W., Drickamer, H.G., *The Effect of Pressure on the Resistance and Lattice Parameters of Cadmium and Zinc*, Journal of Physics and Chemistry of Solids, 26, 63−68, 1965.

[12] Takemura, K., *The Zinc Story under High Pressure*, Journal of Minerals and Materials Characterization and Engineering, 7, 354−372, 2019.

[13] Rai, S., Prajapati, A.K., Yadawa, P.K., *Effect of Pressure on Elastic Constants and Related Properties of Rare-Earth Intermetallic Compound TbNiAl*, Physical Mesomechanics, 26, 495−504, 2023.

[14] Rai, S., Chaurasiya, N., Yadawa, P.K., *Elastic, Mechanical and Thermophysical properties of Single-Phase Quaternary ScTiZrHf High-Entropy Alloy*, Physics and Chemistry of Solid State, 22, 687−696, 2021.

[15] Voigt, W., *Lehrbuch der Kristallphysik (mit Ausschluss der Kristalloptik)*, B.G. Teubner Verlag, Leipzig, Berlin, 978pp, 1928.

[16] Pugh, S.F., *Relations between the Elastic Moduli and the Plastic Properties of Polycrystalline Pure Metals*, Philosophical Magazine, 45, 823−843, 1954.

[17] Prajapati, A.K., Rai, S., Yadawa, P.K., *Pressure Dependent Elastic, Mechanical, Thermo-Physical and Ultrasonic properties of Titanium Boride*, MAPAN- Journal of the Metrology Society of India, 37, 597−609, 2022.

[18] Yadav, C.P., Pandey, D.K., *Pressure dependent ultrasonic characterization of nano-structured w-BN*, Ultrasonics, 96, 181−184, 2019.

[19] Yadawa, P.K., Rai, S., Chaurasiya, N., Prajapati, A.K., *Investigation of intermetallic GdFeAl ternary compound by elastic, thermophysical and ultrasonic analysis*, Eurasian Physical Technical Journal,19, 105−112, 2022.

[20] Prajapati, A.K., Rai, S., Yadawa, P.K., *Theoretical Investigations on Mechanical and Ultrasonic Characteristics of Gallium Nitride Semiconductor under High Pressure*, Emergent Materials, 5, 1985−1993, 2022.

[21] Srivastav, P., Prajapati, A.K., Yadawa, P.K., *Theoretical Investigation on Thermal, Mechanical and Ultrasonic Properties of Zirconium Metal with Pressure*, Physics and Chemistry of Solid State, 24, 549–557, 2023.

[22] Yadawa, P.K., Singh, D., Pandey, D.K., Yadav, R.R., *Elastic and Acoustic Properties of Heavy Rare-Earth Metals*, The Open Acoustics Journal, 2, 61–67, 2009.

[23] Singh, D., Pandey, D.K., Yadawa, P.K., *Ultrasonic wave propagation in rare-earth monochalcogenides*, Central European Journal of Physics, 7, 198–205, 2009.

[24] Clarke, D.R., *Materials selection guidelines for low thermal conductivity thermal barrier coatings*, Surface and Coatings Technology, 163, 67–74, 2003.

[25] Singh, R.P., Yadav, S., Mishra, G., Singh, D., *Pressure-dependent ultrasonic properties of hcp hafnium metal*, Zeitschrift für Naturforschung A, 76, 549–557, 2021.

[26] Yadawa, P.K., *Computational Study of Ultrasonic Parameters of Hexagonal Close-Packed Transition Metals Fe, Co, and Ni,* Arabian Journal for Science and Engineering, 37, 255–262, 2012.

[27] Guechi, A., Merabet, A., Chegaar, M., Bouhemadou, A., *Pressure effect on the structural, elastic, electronic, and optical properties of the Zintl phase KAsSn first principles study*, Journal of Alloys and Compounds, 623, 219–228, 2015.

[28] Ranganathan, S.I., Ostoja-Starzewski, M., *Universal Elastic Anisotropy Index*, Physical Review Letters, 101, 9007-9008, 2008.

[29] Jaiswal, A.K., Yadawa, P.K., Yadav, R.R., *Ultrasonic wave propagation in ternary intermetallic CeCuGe compound*, Ultrasonics, 89, 22–25, 2018.

[30] Saadi, B., *First-principles calculations to investigate structural, electronic, half-metallic and thermodynamic properties of hexagonal UX_2O_6(X=Cr, V) compounds*, Journal of Science: Advanced Materials and Devices, 4, 319–326, 2018.

[31] Srivastav, P., Yadav, A., Yadawa, P.K., *Theoretical Investigation of the Mechanical and Thermophysical Properties of Mechanoluminescence Material with Partial Replacement of Li in $Li_xZn_{1-x}O$: Nd^{3+} ($0 \leq x \leq 0.44$)*, Ukrainian Journal of Physics, 70(11), 805–813, 2025.

[32] Gray, D.E., *AIP Handbook*, 2nd ed., McGraw-Hill, New York, USA, 2112p., 1963.